

α_S from Υ Spectroscopy with dynamical Wilson Fermions

SESAM-Collaboration

A. Spitz^{a,b*}, H. Hoerber^a, N. Eicker^{a,b}, S. Güsken^a, Th. Lippert^a,

K. Schilling^{a,b}, T. Struckmann^a, P. Ueberholz^a, J. Viehoff^b

^a*Fachbereich Physik, Bergische Universität Wuppertal,*

D-42097 Wuppertal, Germany

^b*John von Neumann-Institut für Computing,*

Forschungszentrum Jülich, D-52425 Jülich, Germany

(11.06.1999)

Abstract

We estimate the QCD coupling constant from a lattice calculation of the bottomonium spectrum. The second order perturbative expansion of the plaquette expectation value is employed to determine α_S at a scale set by the 2S-1S and 1P-1S level splittings. The latter are computed in NRQCD in a dynamical gauge field background with two degenerate flavours of Wilson quarks at intermediate masses and extrapolated to the chiral limit. Combining the $N_f = 2$ result with the quenched result at equal lattice spacing we extrapolate to the physical number of light flavours to find a value of $\alpha_{\overline{\text{MS}}}^{(5)}(m_Z) = 0.1118(17)$. The error quoted covers both statistical and systematic uncertainties in the scale determination. An additional 5% uncertainty

*email:spitz@theorie.physik.uni-wuppertal.de

comes from the choice of the underlying sea quark formulation and from truncation errors in perturbative expansions.

I. INTRODUCTION

A precise knowledge of the strong coupling constant is of central importance both for strong-interaction phenomenology and for stringent tests of the standard model as a whole. There has been significant progress in determining α_S and its running during the last years: Measurements are available for a large number of different reactions covering energies up to 190 GeV. Although ‘the’ global average has remained nearly unchanged the uncertainties of single measurements as well as the scatter between them has been strongly reduced. The clustering of results into groups of high-energy and low-energy data which was observed back in 1995 has completely disappeared and the various results now nicely align around an average of $\alpha_{\overline{\text{MS}}}(m_Z) \sim 0.119$ [1]. While the majority of determinations of the strong coupling relies on perturbative expansions of high-energy cross sections, lattice simulations of QCD provide, in principle, a nonperturbative access to determine α_S from low-energy quantities (a review of lattice methodology is presented in [2]). In fact, a viable scheme along these lines has been demonstrated with the Schrödinger functional technique in the context of the quenched approximation, $N_f = 0$ [3]. An alternative approach is to consider perturbative expansions of suitable short-distance quantities and to determine their vacuum expectation values from simulations. In this manner Monte Carlo data can be utilized to extract estimates for α_S at a scale which is provided by the lattice spacing, a [4]. This procedure lends itself easily to the setting of full QCD, given that sufficient samples of QCD vacuum configurations are available as demonstrated some time ago in ref. [5]. In the meantime, the statistical precision of the resulting lattice estimates of α_S in $N_f = 0$ and 2 theories has been increased such as to allow for an extrapolation in the number of dynamical flavours to $N_f = 3$.

Although, a priori, any mass or energy splitting calculated in a lattice simulation can be

used to set the lattice spacing, a , in practice one clearly prefers those choices which are least prone to systematic errors. Spin-averaged radial and orbital angular momentum splittings in heavy quarkonium bound states, in particular in bottomonium, are favourite candidates [6]. They are largely insensitive to the heavy quark mass: experimentally one finds the spin-averaged mass splittings between 1P and 1S levels as well as 2S and 1S levels to be nearly equal for the Υ and Ψ bound states. Moreover, one may infer phenomenologically, that they depend only mildly on the light quark masses: assuming characteristic gluon momenta exchanged between quarks inside the Υ to be $O(1\text{GeV})$, heavy flavours will be negligible in virtual quark loops whereas the masses of light quarks are equally small compared to this momentum scale so that their exact values as well as the differences between non-strange and strange quark masses are likely to be of little importance. These arguments imply that (a) there is no need to tune the bare heavy quark mass precisely and (b) to a good approximation the contribution of light quarks can be mimicked by considering three light flavours of average mass [7]. The latter feature is a major benefit in lattice simulations which are technically restricted to rather large quark masses and generally rely on chiral extrapolations.

The *bonus* in choosing spin-averaged level splittings in bottomonium to set the scale stands against the *malus* that the direct simulation of heavy quark dynamics employing standard relativistic actions suffers from serious discretization errors. Among several alternatives to circumvent this problem, the nonrelativistic effective theory for QCD (NRQCD) [8] provides the most appropriate technique for simulating systems containing a b-quark. The NRQCD Lagrangian is written as a series of operators ordered according to powers of the mean-squared heavy-quark velocity. Each operator introduces a new coupling constant which is determined by perturbatively matching the theory to QCD. The decoupling of quark and antiquark fields in NRQCD is equivalent to integrating out the heavy quark mass and, as a consequence, the amount of lattice spacing errors is governed by the characteristic momentum exchanged between heavy quarks, $O(a\Lambda_{\text{QCD}})$, rather than by the underlying quark mass scale.

The realistic inclusion of vacuum polarization effects constitutes a serious hurdle in today's lattice simulations of QCD, in particular for Wilson fermions. One should remember, that the state-of-the-art updating algorithms require an even number of degenerate sea quarks. As a consequence the strong coupling cannot be determined on field configurations with three kinds of active sea quarks, u , d , s ; rather one has to resort to an extrapolation in the number of active flavours. Using the staggered discretisation for the dynamical fermions, Davies and coworkers [5] presented a careful analysis of α_S (including the various sources of error). Consistent results, although with substantially larger errors, have been quoted by the authors of [9,10] who also use staggered sea quarks but heavy Wilson valence quarks instead of nonrelativistic quarks.

In this paper, we shall apply the methods of [5] to the case of dynamical Wilson fermions. They carry different finite- a errors (compared to staggered fermions) that affect both the nonperturbative results for the bottomonium splittings and the plaquette expectation value as well as the perturbative expansion of the plaquette. We shall improve on previous error analyses by studying the quark mass dependence of quarkonium splittings; hence we shall be able to reduce the uncertainty due to the light quark mass scale.

The paper is organized as follows. In Sec. II we briefly recall the set-up of SESAM's hybrid Monte Carlo simulation of lattice QCD with dynamical Wilson fermions as well as the relevant issues of the computation of nonrelativistic propagators from a lattice NRQCD action. We proceed with a presentation of spectroscopy results in Sec. III. Since within the Υ system the singlet states η_b and h_b have not been observed in experiment yet, we have to deviate from the suggestion to use fully spin-averaged splittings and have to choose $2^3S_1 - 1^3S_1$ and $^3\bar{P} - 1^3S_1$ to determine the lattice spacing. Here, $^3\bar{P}$ denotes the spin average of 3P_J . Therefore the discussion of fit results and systematic errors in Sec. III covers radial splittings as well as spin splittings. In Sec. IV we determine the quenched and unquenched plaquette couplings and perform the extrapolation in N_f . We conclude in Sec. V with a discussion of the resulting value of α_S in the continuum $\overline{\text{MS}}$ scheme.

II. SIMULATION SET-UP

The present work is based on ref. [11] and can be described as the final analysis of SESAM lattices with increased statistics, both with respect to the number of configurations and NRQCD propagator inversions, to reduce the error.

A. Gauge Fields

We have performed a hybrid Monte Carlo simulation of full QCD at $\beta = 5.6$ with two degenerate flavours of dynamical standard Wilson fermions. A single lattice size of $L^3 \times T = 16^3 \times 32$ is used. It corresponds to a physical box of 1.2-1.4 fm in the spatial direction (depending on the experimental quantity used to set the scale) which is sufficiently large to exclude finite volume effects on the bottomonium ground state and the first radial and orbital angular momentum excitation. We generated configurations at three different values of the sea quark hopping parameter, κ , each sample consisting of 5000 trajectories from which 200 decorrelated vacuum configurations are chosen. Table I lists the simulation parameters. For details of the HMC run and subtleties concerning autocorrelation studies we refer the reader to [12]. The quenched run uses an overrelaxed Cabbibo-Marinari heat bath update, thermalised with 2000 sweeps, and measurements are performed on configurations separated by 250 sweeps.

B. Some NRQCD Prerequisites

Compared to our intermediate results presented in [13], we have significantly increased our statistics at $\kappa = 0.1575$ and $\kappa = 0.1570$ corresponding to the two lighter quark masses. Heavy quark propagators are calculated in the nonrelativistic approximation. We have implemented the NRQCD action at ‘next-to-leading order’ with spin-independent operators of $O(m_b v^2)$, $O(m_b v^4)$ and spin-dependent terms of $O(m_b v^4)$ and $O(m_b v^6)$ included. The radiative corrections to the coefficients of these interaction terms are not exactly accounted

for. Rather we use the mean field prescription to cover their main effect and choose the tadpole parameter computed from the mean link in Landau gauge. Unlike for light hadrons, in lattice simulations of heavy quarkonium bound states one can efficiently increase statistics by computing propagators from different, widely separated source points on the same configuration. Hence we have averaged the data from up to 12 point sources for the $N_f = 2$ lattices. Note, that we do not use a multi-source, but evolve each starting point separately. In the quenched runs we restrict ourselves to 4 source points as new configurations can be generated with comparatively little effort. To project on radially excited and orbital angular momentum states some care is needed in choosing an appropriate smearing procedure. The method of choice for bottomonium is a fixed-gauge wavefunction smearing technique. For the Υ and η_b we calculate a 4×4 matrix of correlators with four different smearings at source and sink, $sc/sk = l, 1, 2, 3$, corresponding to a point source (1), the ground state (1), the first (2) and second (3) excited states, respectively. For the $L = 1$ states we restrict ourselves to the ground state and the first excitation as signals deteriorate. The smearing functions that we use are the wavefunctions calculated in Ref. [14]. With all the coefficients in the action set to their tree level values the only parameter left besides the gauge coupling is the bare heavy quark mass, am_b . We did not tune the bare b-quark mass but kept $am_b = 1.7$ throughout the simulation. This value reproduces the correct Υ mass in the quenched approximation [13] and it turns out to be adequate in the full theory, too, leading to kinetic masses $m_{\text{kin}}(\Upsilon) = 9.97(28), 9.63(24), 9.68(27)$ GeV for $\kappa = 0.1560, 0.1570, 0.1575$, respectively.

III. BOTTOMONIUM SPECTROSCOPY

A. Fit Results

We determine the triplet-S state 1^3S_1 and its first radial excitation as well as the singlet-P ground state 1^1P_1 by a simultaneous fit of two source-smearred correlators to a double-

exponential ansatz

$$C_{sc,l}(T) = b_{sc,l}^1 e^{-aE_1 T} + b_{sc,l}^2 e^{-aE_2 T} \quad sc = 1, 2 . \quad (1)$$

These fits yield the cleanest signals and are very stable. We varied the fit interval over a considerable range as illustrated in Fig. 1 for the sample with the lightest sea quark content. The analysis reveals clear plateaus in global masses for each meson correlator. Since fits to smeared-local correlators usually tend to overestimate the plateau value, we have varied the fitting procedure to check for the stability of the results. First, we have used correlators which are smeared both at source and sink in a two-exponential fit. Sink smearing produces noisier signals. Nevertheless, ground state energies are obtained with similar accuracy and yield consistent results. Excited states, however, exhibit significantly larger errors compared to the smeared-local data. Second, we have applied fits involving two smeared-local correlators but three exponentials. The third exponential is meant to account for contaminations from higher radial excitations and to provide a more reliable estimate of the 2S state. The results are in very good agreement with those obtained from two exponentials, thus providing confidence in the radially excited level. Since both singlet resonances, η_b and h_b , have not been observed experimentally we have to recourse to the known splittings $2^3S_1 - 1^3S_1$ and $\bar{P} - 1^3S_1$ to set the lattice scale. Here, \bar{P} denotes the spin-average triplet-P state: ${}^3\bar{P} = \frac{1}{9} ({}^3P_0 + 3 \cdot {}^3P_1 + 5 \cdot {}^3P_2)$. To obtain ${}^3\bar{P}$ we have to determine the P fine structure which is accomplished by single exponential fits to the ratio of two correlators

$$C_1(T)/C_2(T) = A \exp(-\Delta E_{12} T) , \quad \Delta E_{12} = E_1 - E_2 . \quad (2)$$

This way we compute the splittings of 3P_J relative to 1P_1 for $J = 0, 1, 2$ which are then combined to form the spin average. In the case of smeared-local correlators the plateau sets in only at rather large times. For P-wave states these can hardly be reached before the signal is drowned into noise. Results quoted for spin splittings have therefore been taken from smeared-smeared correlators. These run into plateaus at early times where they

differ considerably from their smeared-local counterparts as illustrated in Fig. 1. Table II summarizes the relevant fit results. Errors are taken from 300 bootstraps.

B. Extrapolation in the light quark mass

The hopping parameters that we have chosen correspond to quark masses in the range $m_s/2 \leq m_q \leq m_s$ where m_s denotes the strange quark mass. According to [15] one expects the energy splittings to depend linearly on the light quark mass, m_q , in lowest order of a chiral expansion. Hence we choose the simple ansatz

$$a\Delta E = a\Delta E_0 + c am_q \quad (3)$$

to extrapolate in m_q . As illustrated in Fig. 2 the splittings considered here exhibit a very mild dependence on the sea quark mass. In fact, one cannot distinguish their values at $a\tilde{m} \equiv am_s/3 \sim 0.0159$ and our smallest simulated mass.¹ As outlined in the introduction \tilde{m} is a reasonable average quark mass provided the strange-nonstrange mass difference can be neglected for the lowest Υ bound states. If extrapolated down to the physical light quark mass the splittings increase modestly. The parameters of uncorrelated linear fits are listed in Table III together with the splittings at \tilde{m} and m_l . We conclude that within the accuracy of our data no deviation from linear behaviour is found and we emphasize that sea quark mass dependences are smaller by one order of magnitude compared to the light hadron sector [12].

We may choose the difference in mean values of $a\Delta E(m_s/3)$ and $a\Delta E(m_l)$ as an upper limit of the uncertainty in the sea quark mass: $1^3\bar{P} - 1^3S_1$ exhibits a 4% decrease, whereas $2^3S_1 - 1^3S_1$ is affected by 7%. From the experimental bottomonium splittings $\Upsilon' - \Upsilon = 0.5629$ GeV and $\bar{\chi} - \Upsilon = 0.4398$ GeV one determines the lattice scales summarized in Table IV. We use the average value of a^{-1} at \tilde{m} to convert our lattice results into physical units.

¹Note that κ_s determined using the K mass disagrees with the value calculated from K^* or Φ . We use an average here since the exact value of κ_s is clearly not important in the present analysis.

As intended, it matches the (mean) value of the quenched lattice spacing at $\beta = 6.0$, so that unquenching effects can be studied.

It is obvious from Fig. 3 that the quenched spectrum does not reproduce the experimental spectrum while the $N_f = 2$ data is in much closer agreement. This behaviour can be ascribed to the different running of the coupling in both theories and translates into a discrepancy between the plaquette coupling as determined from the 2S-1S and 1P-1S splittings in the quenched approximation as we shall see below.

C. Error Estimates

Besides the dependence on the sea quark mass several error sources deteriorate the accuracy of the energy splittings and hence affect the precision in scale determination:

Inherent to the nonrelativistic approach one is faced with higher order relativistic corrections due to the truncation of the effective NRQCD Lagrangian of choice and to the incomplete renormalization of coefficients in the velocity expansion. Having included spin-independent terms through $O(m_b v^4)$ we expect that spin-averaged splittings will receive a 1% correction from higher orders (interactions of $O(m_b v^6)$). But this is just the order of magnitude incurring by second-order spin-dependent effects! Hence we may estimate the truncation error by switching off the latter. By inspection of Table V we find that this procedure leaves the energy levels unaltered. A ratio fit to the S hyperfine splitting, however, reveals a 15% decrease when $O(m_b v^6)$ interactions are switched on as is expected from power counting. The impact of the incomplete renormalization of the NRQCD expansion coefficients is exposed by changing the tadpole improvement factor from the Landau-link prescription, $u_0^L \equiv \langle \frac{1}{3} \text{Tr} U_\mu \rangle_{\text{LG}}$, to the plaquette prescription, $u_0^P \equiv \sqrt[4]{\langle \frac{1}{3} \text{Tr} U_{\mu\nu} \rangle}$. It turns out to be of similar magnitude. As a conservative estimate, we shall henceforth quote an additional error of 0.10 in a^{-1} to cover both effects and refer to it as the uncertainty in the NRQCD expansion.

We have explicitly calculated the dependence of the 2S-1S radial splitting on the bare

heavy quark mass. Of course, we expect very little change as we vary am_b . This is indeed confirmed as can be seen from Fig. 4, where we plot the triplet S radial splitting as a function of kinetic mass. The latter is computed for each bare mass value, $am_b = 1.6 - 2.0$, by giving the meson a small amount of momentum and fitting the nonrelativistic dispersion relation.

We have not checked for finite volume effects. We expect them to be much smaller for quarkonia than for light mesons. Quenched lattices of size ~ 1.5 fm are found to be sufficient for the lowest charmonium levels [5]. Hence our results for 2S-1S and 1P-1S in bottomonium are safe. But, as pointed out in [16], higher radial excitations like 2P or 3S require a linear lattice extent larger than 2 fm, even for bottomonium.

Finally, our results will be affected by various finite- a errors. Note, that these cannot be removed by extrapolation, since there exists no continuum limit to NRQCD. Instead the latter should be viewed as being based on an effective action that is geared to obtain physical results *at finite cut-off* only. Obviously, in order to make sure that the effective action approach is a useful tool one has to ascertain that the spectrum is independent of the lattice spacing within a certain window. This then would establish that the matching of the NRQCD action to QCD is sufficiently accurate.

For nonrelativistic b-quarks discretization errors are likely to be larger than in the light hadron spectrum. The improvement of the NRQCD Lagrangian is thus a crucial issue and its efficiency has to be checked explicitly by simulating at different values of β . We have removed $O(a^2)$ errors in the tree approximation, but we cannot perform a scaling analysis for the dynamical data, as we are restricted to a single lattice spacing. In the quenched approximation Davies et. al. [17] have studied the bottomonium spectrum on three quenched lattices with spacings in the range 0.05 fm to 0.15 fm. They find good scaling in the ratio of radial and orbital $b\bar{b}$ splittings to the ρ -mass if the latter is computed from a tadpole improved clover action. Also ratios of such splittings within the Υ -system do not exhibit any dependence on the lattice spacings (spin splittings do!). Although these results are quite encouraging, we emphasize that dynamical Wilson fermions introduce additional linear

scaling violations whose size can only be safely estimated through simulations at different lattice spacings.

IV. PLAQUETTE COUPLING

A value of the strong coupling now is readily obtained: compute the expectation value of a short distance quantity on the lattice and match it with the perturbative expansion. Obviously, this is a reasonable procedure only, if nonperturbative effects are negligible which is definitely the case for the simplest lattice quantity, the 1x1 Wilson loop. While the common choice of the expansion parameter in the continuum is the $\overline{\text{MS}}$ -coupling, on the lattice it is more suitable to choose a subtraction scheme that refers to a nonperturbative quantity like the static $Q\bar{Q}$ -potential [18]. Rather than using α_V itself we adopt here a slightly modified scheme, defined in Ref. [5] through

$$-\ln\langle\frac{1}{3}\Re\text{Tr}U_{\mu\nu}\rangle = \frac{4\pi}{3}\alpha_P\left(\frac{3.41}{a}\right) [1 - (1.1870 + 0.0249 N_f)\alpha_P] , \quad (4)$$

the rationale behind this definition of plaquette coupling, α_P , being a matter of convenience: one has to worry about higher order perturbative corrections only once, when converting the lattice coupling into a standard continuum scheme at the very end of the analysis. Note that Eq. 4 is valid in the chiral limit and for Wilson fermions. One prefers to expand the logarithm of the plaquette since it converges more rapidly than the plaquette expectation value itself. The scale $3.41/a$ is the ‘average gluon momentum’ in the first-order contribution to $-\ln W_{11}$ computed with the technique suggested in [19]. In Table VI we summarise the couplings α_P obtained from Eq.(4) as well as the scales determined from the 1P-1S ($\bar{\chi} - S$) and 2S-1S ($\Upsilon' - \Upsilon$) splittings.

In the unquenched case we quote values for both $am_q = am_s/3$ and $am_q = am_l$ to estimate the systematic error connected to the finite sea-quark mass. Plaquette expectation values have been extrapolated accordingly. We do not quote an error for them since it is negligible compared to the uncertainty in the scale. Subsequently these couplings are evolved

to a common scale $\mu = 9.0$ GeV using the universal two-loop β function, see Table VII. The error in the evolution is minute as the evolution range is very small. For instance, using just the one-loop evolution results in a deviation of much less than 1%.

The plaquette couplings in the quenched and unquenched theories can now be extrapolated to the number of active light quark flavours which is expected to be $N_f = 3$ in the case of the low-lying $b\bar{b}$ bound states. Guided by the perturbative evolution, we extrapolate α_P^{-1} linearly in N_f , Figure 5. Obviously the mismatch between α_P -values obtained from different splittings in the quenched approximation disappears, once the dynamical quarks are switched on. Thus we find, that full QCD with Wilson fermions shows similar behaviour as QCD with staggered dynamical fermions [5]. Nevertheless, there is no way to pin down the the number of active flavours precisely. Continued extrapolation to $N_f = 4$ further increases α_P (with the error blown up) and leads to 1σ increase in $\alpha_{\overline{\text{MS}}}(M_Z)$. Hence simulations with $N_f > 2$ are called for to reduce this uncertainty.

Consider once more the ordering of extrapolations that have been performed to arrive at $\alpha_P^{(3)}$. First we have extrapolated splittings in lattice units as a function of the dynamical quark mass to determine a^{-1} at \tilde{m} . Then we performed the N_f -extrapolation. One might argue about this prescription of carrying out the limits. Alternatively one might prefer to do the flavour extrapolation at fixed quark mass. Although in principle at finite lattice spacing the order may matter, we see no difference: the couplings separately obtained at each sea-quark mass, see Table VIII, do not reveal any significant dependence on m_q and are consistent with those in Table VII.

V. DISCUSSION

To make the connection with the $\overline{\text{MS}}$ -scheme one invokes

$$\alpha_{\overline{\text{MS}}}^{(N_f)}(Q) = \alpha_P^{(N_f)}(e^{5/6}Q) \left[1 + \frac{2}{\pi} \alpha_P^{(N_f)} + C_2(N_f)(\alpha_P^{(N_f)})^2 + O((\alpha_P^{(N_f)})^3) \right], \quad (5)$$

with a scale factor $e^{-5/6}$ chosen to eliminate the N_f dependence in the first-order coefficient of the expansion [20]. The crucial point about Eq.(5) concerns the coefficient C_2 which is

only known in pure gauge theory and thus causes a significant uncertainty on $\alpha_{\overline{\text{MS}}}$. Let us, for the moment, ignore this uncertainty and set $C_2 \approx 0.95$, as in the quenched theory, to study the errors directly related to the lattice method. We start from $\alpha_P^{(3)}(9.0 \text{ GeV})$ and evolve the coupling to the Z meson mass scale, applying the formulae in [21]: First, $\alpha_{\overline{\text{MS}}}^{(3)}(e^{-5/6} \cdot 9.0 \text{ GeV})$, is evolved down to the charm threshold with the three-loop beta function. Matching the three flavour with the four flavour theory, one obtains $\alpha_{\overline{\text{MS}}}^{(4)}(M_c)$ which in turn is evolved upwards to the b-quark threshold. We have chosen $m_c = 1.3 \text{ GeV}$ and $m_b = 4.1 \text{ GeV}$ for the charm and bottom thresholds, see Table IX. As was already noted in [22], the value of the coupling at m_Z is insensitive to the precise location of the matching point. Errors are propagated by performing the evolution on each bootstrap sample separately. They turn out to exceed the effect of this matching procedure by an order of magnitude. As a result we obtain the consistent estimates

$$\alpha_{\overline{\text{MS}}}^{(5)}(m_Z) = \begin{cases} 0.1118 \text{ (10)(12)(5)} & \text{from } \bar{\chi} - \Upsilon \text{ splitting} \\ 0.1124 \text{ (13)(12)(15)} & \text{from } \Upsilon' - \Upsilon \text{ splitting} \end{cases} \quad (6)$$

We give three errors to quantify the uncertainty in the lattice scale determination: the statistical error, the systematic error of the NRQCD expansion and the uncertainty originating from the sea-quark mass dependence. eq.6 permits the following conclusions: we have attained statistical errors on the level of the systematic uncertainties, hence they are not the limiting factor, even in the unquenched theory. In addition, the errors induced by applying nonrelativistic QCD and unphysically heavy sea quarks appear to be fairly well under control.

One might be tempted to grade eq. 6 as a “high precision” determination of α_s : Adding the errors quadratically, one finds in fact an overall uncertainty of “only” $\sim 1.5\%$, which is quite small compared to the errors found in recent experimental measurements of the strong coupling [23].

This conclusion, however, might be misleading. Recall that our analysis has been performed within a fixed (Wilson) discretization scheme, at a given value of the lattice cutoff a^{-1} , and with an incomplete conversion prescription $\alpha_{\overline{\text{MS}}}^{(N_f)}(\alpha_P^{(N_f)})$, c.f. eq.5. Clearly, system-

atic effects which might arise from these limitations can be taken into account properly only by variation of the setup.

To estimate the size of these additional uncertainties we compare our results with those of ref. [5]. The latter analysis has been done at a similar value of the lattice cutoff, with the same conversion prescription $\alpha_{\overline{\text{MS}}}^{(N_f)}(\alpha_P^{(N_f)})$, but within the Kogut Susskind discretization scheme. As their final result, the authors of ref. [5] quote $\alpha_{\overline{\text{MS}}}^{(5)}(m_Z)$ to be 0.1174(15) and 0.1173(21) from the $\bar{\chi} - \Upsilon$ and $\Upsilon' - \Upsilon$ splitting, respectively. These values exceed our result by 5% or three sigmas! Thus, one concludes that the “true” systematic uncertainty is 3 to 4 times larger than the one given in eq. 6².

Let us discuss the possible origins of the additional uncertainty in some more detail:

(1) Both, the errors caused by the unknown flavour dependence of C_2 and the truncation of the perturbative series, Eq. 5, have been ignored up to now. To estimate their magnitude we vary the N_f -dependent part of C_2 within a reasonable range, allowing values between -1 and +1. In addition we set the coefficient of the third-order contribution to unity. The latter turns out to have practically no effect, whereas the variation of C_2 suggests an extra 2-3% uncertainty. It is thus not implausible that the discrepancy in $\alpha_{\overline{\text{MS}}}^{(5)}$ is due to our ignorance on C_2 .

(2) The difference in couplings between Wilson and staggered data is already present prior to converting to the continuum renormalization scheme. We have evolved $\alpha_P^{(2)}$ as it results from our analysis to the momentum scale used in ref. [5] and find $\alpha_P^{(2)}(8.2 \text{ GeV}) = 0.1714(25)$, a 4% difference compared to the staggered result. This deviation can be traced back directly to the difference in plaquette values which is larger than anticipated from the perturbative expansion, while the scales in both simulations are compatible within errors. This signals the presence of sizeable finite-a errors.

²Of course, the same error (5%) should be added to the result of ref. [5] since, from the current stage of knowledge, one cannot tell which discretization scheme yields results closer to the continuum.

Both points constitute substantial limitations.

To reduce the error stemming from source (1) it is of utmost importance to calculate perturbatively the coefficient $C_2(N_f)$ both, for Wilson and for Kogut Susskind fermions.

A reduction of the uncertainty related to source (2) will require a much more detailed numerical analysis. Since the continuum limit $a \rightarrow 0$ does not exist in NRQCD, one cannot remove cutoff effects by extrapolation in a . Instead one has to rely on improved discretization schemes, which avoid sizeable cutoff effects already at finite a . The compelling test however, whether a given scheme really reduces cutoff effects compared to Wilson or Kogut Susskind discretizations can be performed only by a scaling analysis in full relativistic lattice QCD. Thus, in a sense, improvement of NRQCD presupposes the improvement of relativistic lattice QCD with respect to discretization errors.

VI. SUMMARY AND CONCLUSION

Heavy quarkonium bound states are potentially able to reveal the QCD coupling to high precision. Our main objective here has been to acquire a better understanding of the various sources of error when applying NRQCD techniques to carry out this program in lattice QCD. We have been able to reduce statistical errors to the level of systematic effects. Among the latter, uncertainties from the truncation of the NRQCD action and the dynamical quark mass dependence are found to be under good control. On the other hand, errors due to flavour extrapolation are more subtle to pin down but seemingly not dominant. Much more relevant is the choice of lattice action for the light quarks. Our analysis, using Wilson quarks, leads to a value of $\alpha_{\overline{MS}}^{(5)}(m_Z)$ significantly smaller than comparable calculations based on staggered light quarks. This suggests that discretization errors do play an important role in limiting the precision of NRQCD type determinations of the strong coupling and suggests to base the analysis on the use of improved Wilson type actions. Needless to say, as a first step, one must improve the perturbative recoupling between the lattice and \overline{MS} schemes.

ACKNOWLEDGEMENTS

We thank the members of the Wuppertal DELPHI group for fruitful discussions. A.S. wishes to thank C. Davies for many helpful suggestions. We appreciate support by EU network Grant No. ERB CHRX CT 92-0051. Computations were done on the Connection Machines CM5 in Wuppertal and Erlangen. We are grateful to the staff of the Rechenzentrum at the University of Erlangen.

REFERENCES

- [1] S. Bethke, hep-ex/9812026, 1998; S. Hahn, hep-ex/9812021, 1998
- [2] P. Weisz, Nucl. Phys., B(Proc. Suppl.) 47, 71-83, 1996
- [3] M. Lüscher, R. Sommer, P. Weisz, and U. Wolff, Nucl. Phys., B413, 481-502, 1994
- [4] A.X. El-Khadra et al, Phys. Rev. Lett., 69, 729-732, 1992
- [5] C.T.H. Davies et al, Phys. Lett. B345, 42, 1995; Phys. Rev. D56, 2755, 1997
- [6] G.P. Lepage, Nucl. Phys. Proc. Suppl. 26, 45, 1992
- [7] J. Shigemitsu, Nucl. Phys. Proc. Suppl., 53, 16, 1997
- [8] G.P. Lepage et al, Phys. Rev. D46, 4052, 1992
- [9] M. Wingate et al, Phys. Rev. D52, 307, 1995
- [10] CP-PACS collaboration, S. Aoki et al, Phys. Rev. Lett., 74, 22, 1995
- [11] A. Spitz, DESY-THESIS-1998-035, Wuppertal University, 1998
- [12] SESAM Collaboration, N. Eicker et. al., Phys. Rev. D59, 014509, 1998
- [13] SESAM Collaboration, N. Eicker et. al., Phys. Rev. D57, 4080, 1997
- [14] G.S. Bali, K. Schilling, and A. Wachter, Phys. Rev. D56, 2566, 1997
- [15] B. Grinstein and I.Z. Rothstein, Phys. Lett. B385, 265, 1996
- [16] G.S. Bali, P. Boyle, hep-lat/9809180, 1998
- [17] C.T.H. Davies et. al., Phys. Rev. D58, 054505, 1998
- [18] L. Susskind, in R. Balian and C.H. Llewellyn Smith (eds.),
Proceedings of the Les Houches Summer School, 1977
- [19] G.P. Lepage and P.B. Mackenzie, Phys. Rev. D48, 2250, 1993

- [20] S.J. Brodsky, G.P. Lepage and P.B. Mackenzie, Phys. Rev. D28, 228, 1983
- [21] G. Rodrigo and A. Santamaria, Phys. Lett. B313, 441-446, 1993
- [22] C.T.H. Davies et. al., Nucl. Phys. 47 (Proc. Suppl.), 409, 1996
- [23] C. Caso et al, The European Physical Journal C3 (1998) 1

TABLES

TABLE I. *Simulation set-up. Where two numbers are quoted they refer to S-wave/P-wave correlators.*

	Dynamical Wilson		Quenched	
	$\beta = 5.6, 16^3 \times 32$		$\beta = 6.0, 16^3 \times 32$	
κ	0.1560	0.1570	0.1575	
m_π/m_ρ	0.833(3)	0.758(11)	0.686(11)	
# configurations	206	192	203	811/520
# point sources	4/4	13/8	12/12	4/4

TABLE II. *Fit results in lattice units. $1^3S_1, 2^3S_1$ and 1^1P_1 are obtained from two-exponential fits to smeared-local correlators, spin splittings are taken from ratio fits to smeared-smeared correlators.*

	$N_f = 2, \beta = 5.6$			$N_f = 0, \beta = 6.0$
Level	$\kappa = 0.1575$	$\kappa = 0.1570$	$\kappa = 0.1560$	
1^3S_1	0.3584(6)	0.3606(6)	0.3652(9)	0.3438(4)
2^3S_1	0.590(8)	0.601(10)	0.631(20)	0.589(12)
1^1P_1	0.530(5)	0.536(6)	0.549(7)	0.508(6)
$1^3P_2 - 1\bar{P}$	0.0034(4)	0.0032(4)	0.0028(4)	0.0032(3)
$1\bar{P} - 1^3P_1$	0.0024(5)	0.0021(5)	0.0018(3)	0.0020(4)
$1\bar{P} - 1^3P_0$	0.0099(10)	0.0096(11)	0.0087(10)	0.0098(5)
$1\bar{P} - 1^1P_1$	0.0003(4)	0.0000(5)	-0.0001(3)	0.0004(3)

TABLE III. Results of the extrapolation in the sea-quark mass. ${}^3\bar{P}$ is the spin-averaged triplet- P state.

splitting	$a\Delta E_0$	c	$a\Delta E(m_s/3)$	$a\Delta E(m_l)$
$2^1S_0 - 1^1S_0$	0.209(21)	1.2(7)	0.229(10)	0.212(19)
$2^3S_1 - 1^3S_1$	0.209(18)	1.1(7)	0.226(9)	0.211(17)
$1^3\bar{P} - 1^3S_1$	0.163(9)	0.4(3)	0.170(5)	0.164(8)
$2^1P_1 - 1^1P_1$	0.152(24)	1.8(7)	0.181(15)	0.156(23)

TABLE IV. Determination of the lattice spacing from the $2^3S_1 - 1^3S_1$ and $1^3\bar{P} - 1^3S_1$ splittings.

	$N_f = 0$	$\kappa = 0.1560$	$\kappa = 0.1570$	$\kappa = 0.1575$	$m_s/3$
$a^{-1}(\Upsilon' - \Upsilon)[\text{GeV}]$	2.29(11)	2.12(16)	2.34(9)	2.43(8)	2.49(10)
$a^{-1}(\bar{\chi} - \Upsilon)[\text{GeV}]$	2.68(9)	2.38(8)	2.50(8)	2.57(7)	2.59(7)

TABLE V. Comparison of quenched Υ and η_b energies obtained with the $O(m_b v^4)$ and $O(m_b v^6)$ actions. Simulation parameters are $\beta = 6.0$, $M_b = 1.7$.

action	u_0	1^1S_0	2^1S_0	1^3S_1	2^3S_1	$1^3S_1 - 1^1S_0$
$O(m_b v^4)$	u_0^L	0.3299(6)	0.581(12)	0.3441(7)	0.587(14)	0.01443(23)
$O(m_b v^6)$	u_0^L	0.3309(4)	0.582(12)	0.3438(4)	0.589(12)	0.01266(8)

TABLE VI. Results for $\alpha_P(3.41/a)$ extracted from the measured plaquette value. We quote the statistical error on the lattice scale as well as the systematic NRQCD error.

β	N_f	M_q	$-\ln\langle\frac{1}{3}\Re\text{Tr}U_{\mu\nu}\rangle$	$\alpha_P^{(N_f)}(\frac{3.41}{a})$	$\frac{3.41}{a}$ [GeV]	
					$\bar{\chi} - \Upsilon$	$\Upsilon' - \Upsilon$
5.6	2	$M_s/3$	0.5570	0.1678	8.84(26)(35)	8.48(33)(32)
	2	M_l	0.5546	0.1668	9.16(45)(70)	9.09(72)(71)
6.0	0	∞	0.5214	0.1518	9.13(34)(37)	7.82(38)(38)

TABLE VII. Plaquette couplings at the reference scale $\mu = 9.0$ GeV. The last two columns are the result of an extrapolation in the flavour number. The first error is statistical, the second is the systematic error within NRQCD.

Splitting	$\alpha_P^{(0)}$ (9.0 GeV)	$\alpha_P^{(2)}$ (9.0 GeV)		$\alpha_P^{(3)}$ (9.0 GeV)	
		$M_q = M_s/3$	$M_q = M_l$	$M_q = M_s/3$	$M_q = M_l$
$\bar{\chi} - \Upsilon$	0.1525(17)(18)	0.1670(14)(19)	0.1677(24)(36)	0.1753(25)(32)	0.1764(41)(62)
$\Upsilon' - \Upsilon$	0.1458(20)(20)	0.1650(18)(17)	0.1673(38)(37)	0.1767(33)(33)	0.1806(69)(68)

TABLE VIII. Plaquette couplings at the reference scale $\mu = 9.0$ GeV for each sea quark mass. Here, we quote only one error, covering both statistical and systematic uncertainties.

κ	$\langle\frac{1}{3}\Re\text{Tr}U_{\mu\nu}\rangle$	$\bar{\chi} - \Upsilon$		$\Upsilon' - \Upsilon$	
		$\alpha_P^{(2)}$ (9.0 GeV)	$\alpha_P^{(3)}$ (9.0 GeV)	$\alpha_P^{(2)}$ (9.0 GeV)	$\alpha_P^{(3)}$ (9.0 GeV)
0.1560	0.5698	0.1651(26)	0.1723(46)	0.1598(39)	0.1679(68)
0.1570	0.5716	0.1661(25)	0.1739(43)	0.1631(26)	0.1733(55)
0.1575	0.5725	0.1667(22)	0.1749(37)	0.1642(26)	0.1753(44)

TABLE IX. $\overline{\text{MS}}$ coupling at the heavy-quark thresholds and the Z mass.

Splitting	$\alpha_{\overline{\text{MS}}}(1.3 \text{ GeV})$		$\alpha_{\overline{\text{MS}}}(4.1 \text{ GeV})$		$\alpha_{\overline{\text{MS}}}(91.2 \text{ GeV})$	
	$M_s/3$	M_l	$M_s/3$	M_l	$M_s/3$	M_l
$\bar{\chi} - \Upsilon$	0.316(9)(11)	0.320(14)(22)	0.2034(33)(44)	0.2050(55)(84)	0.1118(10)(12)	0.1123(16)(24)
$\Upsilon' - \Upsilon$	0.321(12)(9)	0.335(26)(26)	0.2053(45)(37)	0.2106(95)(89)	0.1124(13)(12)	0.1139(27)(28)

FIGURES

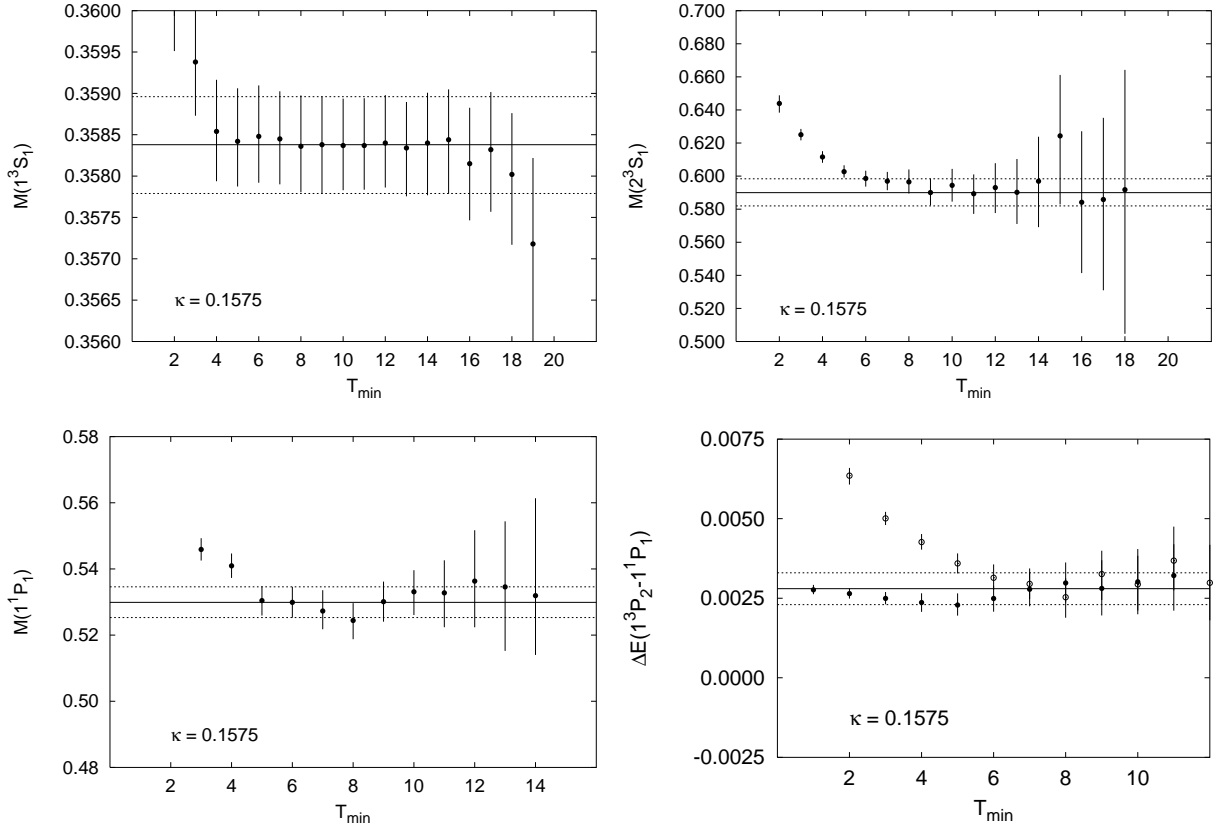


FIG. 1. Global masses as a function of T_{\min} with $T_{\max} = 30$. Lines mark the selected fit value (solid) and its error bands (dotted). For the spin-splitting (lower right plot) smeared-local (open symbols) and smeared-smeared data (filled symbols) are plotted.

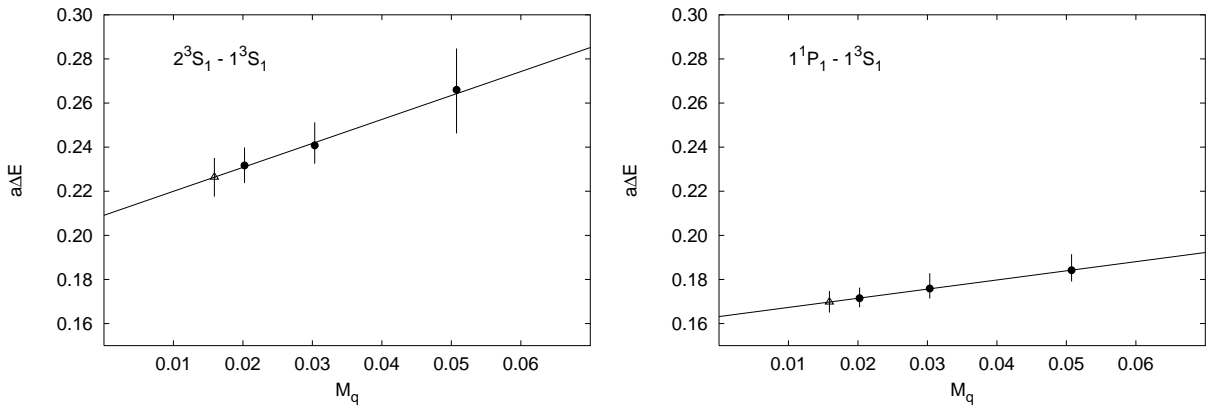


FIG. 2. Extrapolation of the splittings between the Υ ground state and its radial and orbital angular momentum excitation in the dynamical quark mass. The open triangle denotes the value at \tilde{m} .

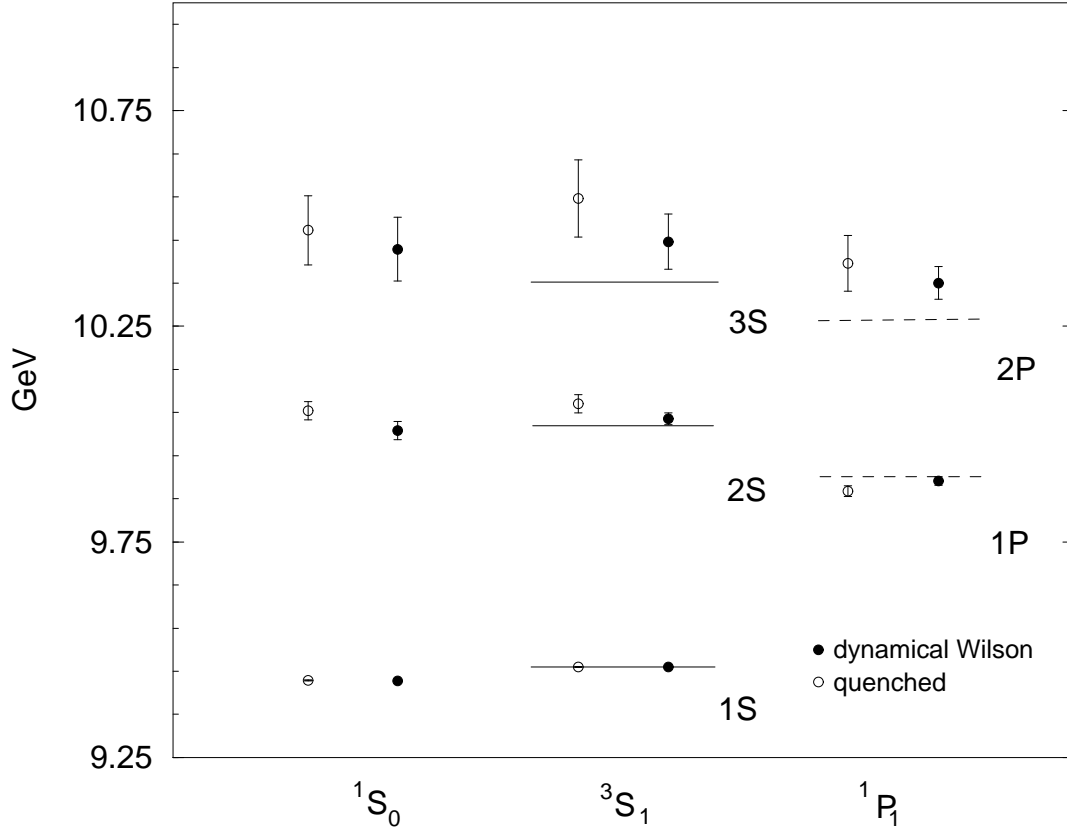


FIG. 3. Bottomonium spectrum - radial and orbital angular momentum splittings. The 3S_1 ground state is constrained to match the experimental Υ energy. Open symbols denote quenched results, filled symbols $N_f = 2$ results at $m_q = m_s/3$. Solid lines mark the experimental values, dashed lines the position of the spin-averaged 3P_J states, which turn out to be nearly identical with the singlet- P estimates.

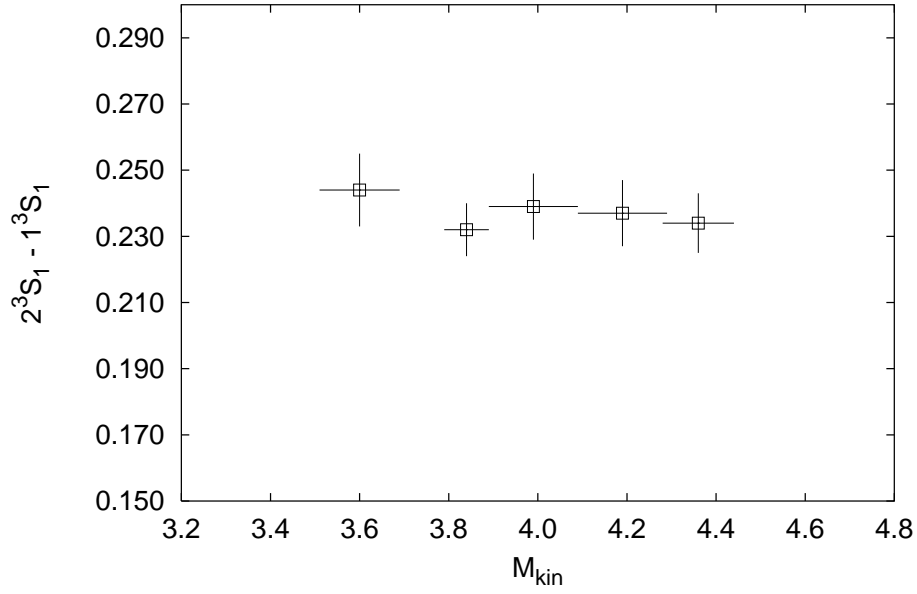


FIG. 4. Dependence of $2^3S_1 - 1^3S_1$ radial splitting on the kinetic mass.

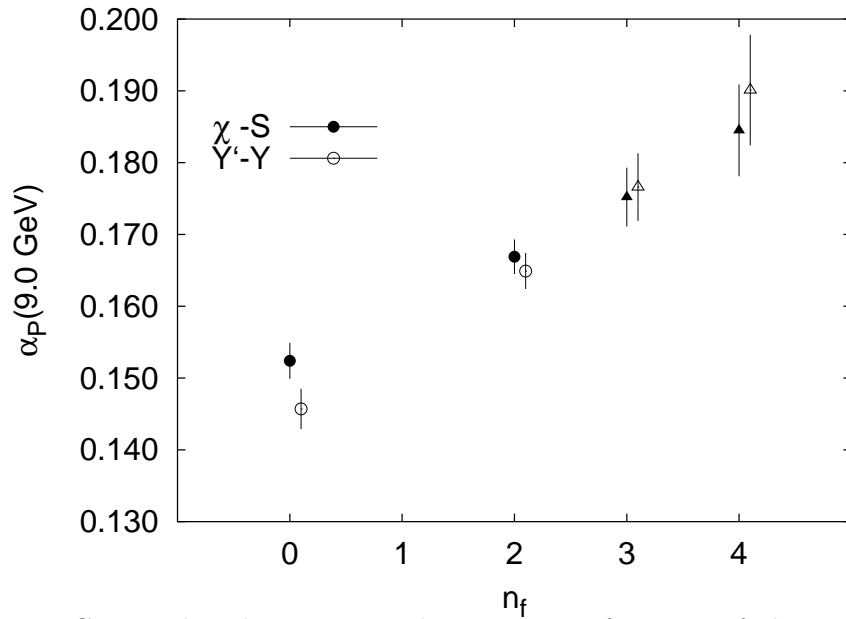


FIG. 5. The plaquette coupling α_P as a function of the number of degenerate dynamical flavours. The triangles result from an extrapolation in the inverse flavour number.